Bull. Minéral.
(1981), **104**, 400-412.

Crystal-chemistry by X-ray structure refinement and electron microprobe analysis of a series of sodic-calcic to alkali-amphiboles from the Nybö eclogite pod, Norway

by LUCIANO UNGARETTI (*), DAVID CHRISTOPHER SMITH (**) and GIUSEPPE ROSSI (*),

(*) C.N.R. Centro di Studio per la Cristallografia Strutturale c/o Istituto di Mineralogia, Via Bassi 4 - 27100 Pavia, Italy
(**) Laboratoire de Minéralogie, Muséum National d'Histoire Naturelle, 61, rue de Buffon, 75005 Paris, France.

Abstract. – The structures of 21 amphibole crystals from a single 16 cm thick compositionally-layered sample from the Nybö eclogite pod, Norway, have been refined by X-ray diffraction. Most compositions lie between winchite and the two end-members which are the most substituted Fe-free amphiboles away from tremolite : $NaNa_2Mg_3Al_2Si_7AlO_{22}(OH)_2$ (nyböite) and $NaCaNaMg_3Al_2Si_6Al_2O_{22}(OH)_2$ (magnesio-alumino-taramite); compositions close to this taramite end-member have not previously been recorded. The main compositional relationships can be explained by a combination of local bulk chemical control, pressure-temperature conditions and crystal-chemical reasoning. Many strong linear correlations occur between unit cell dimensions, bond distances and site occupancies, thus enabling approximate site occupancy determinations from unit cell dimensions alone. Chemical analyses by structure refinement without chemical constraints are comparable in accuracy to chemical analyses of the same crystals using an electron microprobe.

Key words : Crystal-chemistry, sodic amphiboles, eclogite, Norway, X-ray structure refinement, nyböite, taramite.

Étude de la cristallochimie au moyen de l'affinement aux rayons X de la structure et à la microsonde électronique d'une série d'amphiboles sodiques-calciques à alcalines provenant de la lentille d'éclogite de Nybö.

Résumé. – L'affinement aux rayons X de la structure a été réalisé sur 21 amphiboles d'un échantillon lité de 16 cm d'épaisseur provenant de la lentille d'éclogite de Nybö en Norvège. La majorité des compositions ainsi déterminées varient entre winchite et deux pôles qui sont les amphiboles sans fer les plus substituées par rapport à la trémolite : $NaNa_2Mg_3Al_2Si_7AlO_{22}(OH)_2$ (nyböite) et $NaCaNaMg_3Al_2Si_6Al_2O_{22}(OH)_2$ (magnésio-alumino-taramite); aucune composition proche de ce pôle de taramite n'a été signalée jusqu'à présent. Les relations principales des compositions peuvent être expliquées par une combinaison du contrôle par le chimisme global local, des conditions physiques et d'un raisonnement cristallochimique. On observe de nombreuses et bonnes corrélations linéaires entre les dimensions de la maille, la longueur des liaisons, et le remplissage des sites; ce qui offre la possibilité d'une détermination approximative du remplissage des sites avec seulement les dimensions de la maille. Les analyses chimiques effectuées par affinement de la structure sans données chimiques préalables fournissent des résultats comparables à ceux obtenus sur les mêmes cristaux à la microsonde électronique.

Mots clés : Cristallochimie, amphiboles sodiques, éclogite, Norvège, affinement aux rayons X de la structure, nyböite, taramite.

1. INTRODUCTION

The Nybö eclogite pod, Nordfjord, Norway, which is tectonically enclosed within amphibolite-facies country-rock gneisses, is notable for its extreme range of clinopyroxene compositions ($0.0 \leqslant X_{Na}(*) \leqslant 0.82$) as well as the unique occurrence of jadeite-rich acmite-poor omphacites (Smith, 1976; Lappin and Smith, 1978; Smith *et al.*, 1980; Carpenter and Smith, 1981; Rossi *et al.*, 1980). It is equally notable for its extreme range of amphibole compositions ($0.11 \leqslant X_{Na} \leqslant 0.91$; this paper and unpublished data) as well as the unique occurrence of a new Na- and Al-rich amphibole, nyböite (**) (Smith and Ungaretti, in prep.). These exceptional features, coupled with certain other unusual mineralogical features indicative of a high pressure origin (*e.g.* co-existing magnesite + diopside, a quartz vein formed by pyroxene carbonation, a barroisite pegmatite; Smith, 1976 and unpublished data; Lappin and Smith, 1978 and in press) suggest an exceptional origin for the Nybö eclogite pod, such as tectonic introduction from upper mantle depths (Lappin and Smith, 1978 and in press; Smith, 1976, 1978, 1980 *a*, *b*).

(*) X_{Na} = Na/(Na + Ca) in cation proportions (Smith *et al.*, 1980).

(**) Recognition of this name by the I.M.A. is under consideration; crystal chemical data presented here for the type crystal E2 is reproduced from Smith and Ungaretti (in prep.).

We present here a detailed examination of the amphiboles in a single hand-specimen (number G 230*f*) which reveals the variation $0.48 \leqslant X_{Na} \leqslant 0.91$ in only 16 cm. Single crystals were taken from eight consecutive 2 cm-wide horizons (labelled A-H) for X-ray diffractometry and structure refinement; refined crystals from five horizons were subsequently analyzed with an electron microprobe. This enables us to compare the cation site populations determined by the two independent techniques. Furthermore the dependence of amphibole crystal-chemistry upon the local bulk chemical composition (dominated by > 99.5 % modal clinopyroxene + garnet) can be investigated for a wide range of amphibole compositions at presumably constant pressure (P)-temperature (T) conditions, since their low abundance ($\leqslant$ 0.1 % mode) shows that the bulk chemical composition is not significantly dependent upon the amphiboles.

2. FIELD AND PETROGRAPHIC DATA

The papers referenced in the introduction provide the basic field and petrographic data for the Nybö eclogite pod. In general terms, two distinct generations of amphibole are recognized in eclogite pods (lenses) from the Nordfjord district and the neighbouring Selje and Vartdalsfjord districts: « early » amphibole co-existing in apparent equilibrium with garnet + clinopyroxene in hydrous-eclogite-facies parageneses, and later « symplectitic » amphibole co-existing with plagioclase formed by retrogressive alteration (amphibolitisation) of the early eclogite-facies parageneses to amphibolite-facies parageneses (Smith, 1971; 1976; 1980*a*; Lappin and Smith, 1978 and in press). It is usually a straight forward matter to distinguish the two amphibole types on the basis of the non-symplectitic texture, larger size, paler colour and non-pleochroism of the early amphibole. Lappin and Smith (1978) noted higher Al^{IV}, Al^{VI}, Na, Ti and Fe, and lower Mg in the symplectitic amphiboles in orthopyroxene-eclogites, and attributed these differences to their growth at the expense of the typical eclogite-facies paragenesis clinopyroxene + garnet + rutile. In the case of specimen G 230*f*, the distinction of amphibole generation is not so clear, especially in the case of those crystals plucked directly from the rock; all the crystals from horizons A-E are assumed to be early amphiboles since they were taken from symplectite-free areas, whilst the crystals from horizons F-H are unequivocally symplectitic since they co-existed with plagioclase and secondary clinopyroxene (lower X_{Na}) in vein-like amphibolitised horizons.

3. EXPERIMENTAL TECHNIQUES

3.1. X-ray diffractometry

Unit cell dimensions were measured on 48 crystals mounted on a Philips *PW1100* four-circle diffractometer using the routine LAT available in the *PW 1100* software. 21 crystals with the best diffraction effects were selected for intensity data collection and structure refinement; equivalent monoclinic reflections were measured and a semi-empirical absorption correction (North *et al.*, 1968) has been applied; the θ-range explored was 2-30° with Mo$K\alpha$ radiation. Other technical details are given in table I along with the unit cell dimensions of all the refined crystals.

Sample	*a* (A) ±0.001	*b* (A) ±0.002	*c* (A) ±0.001	β (°) ±0.01	*V* (A^3)	n. of I(obs) I≥5σ(I)	n. of I(measd)	R_{sym} ×100	R_{obs} ×100	R_{all} ×100
A4	9.759	17.921	5.290	104.49	895.6d	1128	1358	1.0	1.8	2.4
A5	9.759	17.925	5.290	104.46	896.11	1087	1358	1.2	2.2	3.0
B3	9.746	17.914	5.286	104.30	894.30	1189	1359	2.9	2.8	3.3
B6	9.752	17.917	5.286	104.28	895.09	1118	1358	1.3	2.0	2.8
C1	9.711	17.850	5.292	104.22	889.19	1117	1350	0.9	1.9	2.5
C3	9.721	17.858	5.291	104.22	890.35	1019	1352	1.9	1.9	2.7
D6	9.697	17.805	5.299	104.21	886.94	866	1344	2.2	1.9	3.6
D7	9.666	17.776	5.297	104.06	882.95	905	1339	1.7	2.0	3.6
D9	9.674	17.787	5.295	104.13	883.59	1004	1336	1.8	2.2	3.1
D18	9.693	17.793	5.295	104.16	885.68	1088	1343	1.1	2.0	2.7
E2	9.665	17.752	5.303	104.11	882.36	1091	1335	2.0	2.3	3.1
E9	9.656	17.774	5.299	104.09	881.98	892	1336	1.7	2.0	3.5
E12	9.634	17.760	5.297	104.06	879.27	986	1331	2.1	2.9	3.9
E13	9.654	17.772	5.300	104.11	881.89	921	1335	1.6	2.0	3.3
E14	9.667	17.784	5.299	104.21	883.15	953	1336	2.8	2.0	3.2
E19	9.677	17.779	5.296	104.17	883.48	1076	1340	1.8	2.2	3.0
E19,1	9.663	17.764	5.294	104.12	881.29	950	1336	1.1	1.9	3.2
E19,3	9.684	17.776	5.297	104.23	883.90	826	1334	1.9	2.0	4.3
F3	9.772	17.853	5.310	104.83	895.57	977	1351	1.4	1.9	3.0
G2	9.778	17.859	5.310	104.82	896.43	993	1358	1.4	2.0	3.2
H2	9.786	17.874	5.312	104.84	898.17	944	1358	2.0	2.0	3.2

TABLE I. — *Selected crystal data.* R_{sym} refers to the agreement between the intensity measurements of equivalent reflections and is expressed as :

$$\sum_{hkl} \sum_{i=1}^{N} \left| I(hkl)_i - \bar{I}(hkl) \right| \Big/ \sum_{hkl} \sum_{i=1}^{N} I(hkl)_i$$

where $I(hkl)_i$ is the i^{th} measurement of the reflection *hkl* and $\bar{I}(hkl)$ is the mean value of the *N* equivalent reflections, R_{obs} and R_{all} are the final conventional discrepancy indices expressed as :

$$\Sigma ||F_o| - |F_c|| / \Sigma F_o.$$

The refinements have been carried out without chemical constraints following the procedure described by Ungaretti *et al.* (1978) and Ungaretti (1980); in particular the neutral atomic scattering factors (International Tables for X-ray Crystallography, 1974) were used and, except for the A site, all the structural sites were considered fully occupied. The initial choice of the scattering factors was : Na and vacancy for A; Ca and Na for M4; Mg and Fe for M1, M2 and M3; Si for T1 and T2. After a few least-squares cycles, the bond distances were calculated and used to estimate the Al content of the T1 and M2 sites; thereafter the Al scattering factor was included with that of Si and Mg respectively. The difference Fourier map calculated after the first few cycles of least-squares clearly revealed the location of the hydrogen atom for all the refined amphiboles. The final cycles were performed with fixed Al, Si occupancy as deduced from the T1-O mean bond distances, with

	A		M4			M1		M2					M3			T1 + T2	
Sample	K	Na	Na	Ca	Fe^{2+}	Mg	Fe^{2+}	Mg	Fe^{2+}	Fe^{3+}	Ti	Al	Mg	Fe^{2+}	Fe^{3+}	Al	Si
A4	0.068	0.313	0.730	1.105	0.165	1.846	0.154	1.130	-	0.144	0.026	0.700	0.845	0.102	0.053	0.600	7.400
A5	0.068	0.354	0.710	1.010	0.280	1.866	0.134	1.194	-	0.170	0.026	0.610	0.869	0.075	0.056	0.630	7.400
B3	0.080	0.220	0.810	1.060	0.130	1.854	0.146	1.154	-	0.190	0.026	0.630	0.865	0.080	0.055	0.417	7.583
B6	0.079	0.238	0.820	1.050	0.130	1.872	0.128	1.220	-	0.200	0.026	0.554	0.871	0.070	0.059	0.362	7.638
C1	0.046	0.395	1.120	0.750	0.130	1.822	0.178	0.800	-	0.186	0.024	0.990	0.813	0.187	-	0.545	7.455
C3	0.046	0.405	1.100	0.820	0.080	1.824	0.176	0.926	-	0.110	0.024	0.940	0.823	0.177	-	0.449	7.551
D6	0.030	0.590	1.400	0.600	-	1.816	0.184	0.570	-	0.135	0.020	1.275	0.811	0.189	-	0.670	7.330
D7	0.027	0.520	1.517	0.453	0.030	1.800	0.200	0.532	-	0.040	0.018	1.410	0.783	0.217	-	0.516	7.484
D9	0.030	0.570	1.562	0.438	-	1.932	0.068	0.340	0.18	0.180	0.020	1.280	0.941	0.059	-	0.538	7.462
D18	0.050	0.575	1.480	0.520	-	1.818	0.182	0.590	-	0.120	0.020	1.270	0.826	0.174	-	0.575	7.425
E2	0.024	0.716	1.674	0.326	-	1.824	0.176	0.320	-	0.235	0.017	1.428	0.800	0.200	-	0.763	7.237
E9	0.024	0.596	1.610	0.390	-	1.872	0.128	0.300	0.10	0.130	-	1.470	0.907	0.093	-	0.610	7.390
E12	0.024	0.676	1.760	0.240	-	1.958	0.042	0.040	0.31	0.140	-	1.510	1.000	-	-	0.590	7.410
E13	0.024	0.630	1.658	0.342	-	1.888	0.112	0.200	0.15	0.170	-	1.480	0.901	0.099	-	0.646	7.354
E14	0.024	0.616	1.530	0.470	-	1.880	0.120	0.240	0.15	0.170	-	1.440	0.890	0.110	-	0.720	7.280
E19	0.024	0.816	1.546	0.454	-	1.858	0.142	0.360	0.12	0.120	-	1.400	0.924	0.076	-	0.814	7.186
E19,1	0.024	0.812	1.588	0.412	-	1.850	0.150	0.300	0.20	0.040	-	1.460	0.954	0.046	-	0.748	7.252
E19,3	0.024	0.790	1.512	0.488	-	1.860	0.140	0.400	0.12	0.120	-	1.360	0.909	0.091	-	0.782	7.218
F3	-	1.000	0.938	1.062	-	1.814	0.186	0.340	-	0.500	0.040	1.120	0.775	0.225	-	1.762	6.238
G2	-	1.000	1.000	1.000	-	1.824	0.176	0.360	-	0.520	0.040	1.080	0.793	0.207	-	1.680	6.320
H2	-	1.000	0.940	1.060	-	1.764	0.236	0.350	-	0.560	0.040	1.050	0.749	0.251	-	1.750	6.250

TABLE II. – *Site populations obtained by X-ray single-crystal diffractometry* expressed per $[O_{22}(OH)_2]$ with

$$\Sigma Si + Al + Mg + Fe + Ti - Fe^{2+}_{M4} = 13$$

K and Ti values for each crystal in a particular horizon were usually taken from the WDS microprobe values in the crystal from that horizon, with values for B3 and B6 deriving from A4, and for G2 and H2 from F3; however the K values for B3, B6 and D18 come from the occupancy refinement without any chemical constraints of the A(2/*m*) split position, and Ti was assumed negligible in E9 to E19,3.

full H occupancy, and letting all the other parameters (atomic co-ordinates, anisotropic temperature factors, A, M4, M1, M2, M3 site occupancies, scale factor and secondary extinction coefficient) free to vary until the shifts were less than the e.s.d. of the corresponding parameters. The threshold between observed and unobserved reflections has been chosen, according to the agreement between equivalent pairs, as $I \geqslant 5\sigma(I)$ since the agreement was always good above this value (Ungaretti, 1980).

Correlation among the refined parameters proved to be ineffective in the refinement results which always converged to the same *R*-factor, site occupancies, atomic co-ordinates and thermal parameters, using different starting models and modifying some of the refined parameters.

The refinements have confirmed, as will be seen below, the high accuracy and precision which can be obtained both in the geometric parameters and in the total numbers of electrons per site. The mean value of the e.s.d. is 0.002 A for bond distances and $0.05e^-$ for the number of electrons determined by the site occupancy refinement.

The final population (shown in table II) has been calculated, from a combination of the scattering power measured in each site, mean bond distances (shown in table III) and charge balance requirements, with a new computer program (CORANF) which is based on the following scheme.

Sample	T1 – O		T2 – O	M1 – O		M2 – O		M3 – O		M4 – O
	obs	calc	obs	obs	calc	obs	calc	obs	calc	obs
A4	1.637	1.636	1.630	2.079	2.081	2.023	2.021	2.084	2.084	2.496
A5	1.637	1.636	1.630	2.079	2.081	2.027	2.027	2.082	2.083	2.499
B3	1.631	1.631	1.630	2.078	2.081	2.026	2.025	2.082	2.083	2.503
B6	1.630	1.630	1.630	2.077	2.081	2.030	2.030	2.081	2.083	2.504
C1	1.633	1.635	1.630	2.081	2.082	1.999	1.999	2.088	2.091	2.498
C3	1.632	1.632	1.631	2.079	2.082	2.004	2.004	2.087	2.090	2.502
D6	1.639	1.638	1.631	2.080	2.082	1.980	1.979	2.094	2.091	2.500
D7	1.633	1.634	1.630	2.081	2.082	1.972	1.971	2.091	2.092	2.501
D9	1.635	1.635	1.629	2.075	2.079	1.982	1.981	2.090	2.085	2.501
D18	1.636	1.636	1.631	2.078	2.082	1.980	1.979	2.092	2.090	2.503
E2	1.642	1.641	1.629	2.079	2.082	1.965	1.965	2.097	2.091	2.498
E9	1.636	1.637	1.631	2.078	2.081	1.967	1.967	2.098	2.087	2.500
E12	1.636	1.636	1.629	2.072	2.079	1.966	1.968	2.097	2.087	2.500
E13	1.638	1.638	1.630	2.078	2.080	1.968	1.967	2.095	2.087	2.499
E14	1.640	1.640	1.629	2.077	2.080	1.970	1.970	2.097	2.088	2.497
E19	1.642	1.642	1.630	2.073	2.081	1.971	1.973	2.102	2.086	2.502
E19,1	1.639	1.640	1.629	2.071	2.081	1.970	1.972	2.102	2.085	2.501
E19,3	1.641	1.641	1.629	2.074	2.081	1.976	1.976	2.099	2.087	2.502
F3	1.673	1.669	1.631	2.085	2.082	1.982	1.980	2.097	2.092	2.484
G2	1.671	1.666	1.632	2.084	2.082	1.986	1.983	2.098	2.092	2.487
H2	1.673	1.668	1.632	2.084	2.083	1.991	1.984	2.098	2.094	2.489

TABLE III. – *Observed and calculated mean bond distances.*

3.2. CORANF computer program

In the absence of chemical information, the elements taken into consideration are : Na, Ca, Mg, Fe^{2+}, Fe^{3+}, Al, Si, O, H. If a chemical analysis is available, the following cations are added : K in the A site, Ti^{4+} in the M2 site, and Mn in the M3 site.

The program first calculates the Al^{IV} content on the basis of the $\langle T1 - O \rangle$ mean bond length (see section 4.1). The inclusion of Al^{IV} allows determination of the total negative charge given by the anionic part $(Si, Al)_8O_{22}(OH)_2$. The total positive charge given by the A + M4 sites is then calculated considering Na (and K, when given by the chemical analysis) occurring at the A site and Ca + Na obtained from the M4 site occupancy refinement; Fe^{2+} is included only when

the split position M4′ (Bocchio *et al.*, 1978; Ungaretti, 1980) is revealed by the difference Fourier map. The total number of positive charges to be neutralized by the octahedral cations (P) is obtained by subtracting the total positive charge of the A + M4 sites from the anionic total negative charge. Values lower than 10 and higher than 12 are considered doubtful and the calculation stops, the program calling for a special intervention. Once a value between 10 and 12 is obtained, the M2 site population is computed by solving the following equation system :

$$\left.\begin{aligned} X + Y + Z &= 1 \\ 12X + 13Y + 26Z &= e(\text{obs}) \\ 2.078X + 1.929Y + 2.031Z &= d(\text{obs}) \end{aligned}\right\} \quad (1)$$

where the first equation corresponds to the assumption of full occupancy; e(obs) is the total number of electrons deduced from the site occupancy and 12, 13, 26 are the atomic numbers of Mg, Al, Fe which are considered possible substituents in M2; d(obs) is the mean M2 − O bond distance given by the refinement and the coefficients of the third equation are the mean bond distances of Mg, Al, Fe^{3+} deduced from the refinements of 26 metamorphic alkali amphiboles (Ungaretti *et al.*, 1978).

If the Ti content is available from the chemical analysis, its contribution to the total M2 occupancy, to e(obs) and to d(obs) (assumed value for ⟨Ti − O⟩ is 1.96 A) is introduced into the equation system. Fe^{2+} is not considered present in the M2 site, at least in the first calculation, on the basis of the fact that M2 is usually the smallest octahedral site and Fe^{2+} is the largest octahedral cation. The solution of the equation system (1) gives the site population for M2 and, consequently, the residual positive charge (Q) to be neutralized by the M1 and M3 sites. $Q = 6$ is the expected value for 2M1 + M3 sites fully occupied by three divalent cations, *i.e.* for complete order of the high charge cations at the M2 site. If Q is significantly less than 6, the M1 and M3 sites are considered occupied only by divalent cations and Fe^{2+} is introduced into the M2 site with a mean bond distance of 2.119 Å and with W occupancy obtained by solving the following equation system :

$$\left.\begin{aligned} X + Y + Z + W &= 1 \\ 12X + 13Y + 26Z + 26W &= e(\text{obs}) \\ 2.078X + 1.929Y + 2.031Z + 2.119W &= d(\text{obs}) \\ 2X + 3Y + 3Z + 2W &= P\text{-}6 \end{aligned}\right\} \quad (2)$$

If the residual positive charge Q, obtained after the solution of the equation system (1), is significantly higher than 6, trivalent cations are introduced into the M1 and/or M3 sites, according to their mean bond lengths calculated by using respectively the values 2.078 and 2.083 for ⟨Mg − O⟩ and 2.119 and 2.125 Å for ⟨Fe^{2+} − O⟩ (Ungaretti *et al.*, 1978); when trivalent cations are introduced into the M1 and/or M3 sites, new bond lengths are calculated considering as Fe^{3+} part of the Fe^{2+} present in M1, M3 sites until a good agreement between observed and calculated mean bond distances is reached. If the total charge imbalance obtained in this way is confined within ± 0.07 charges (a figure which corresponds to the expected error in the Al^{IV} estimate deduced from ⟨T1 − O⟩) the program is allowed to modify the tetrahedral aluminium content in order to obtain a neutral chemical formula. If the total charge imbalance exceeds 0.07 positive charges the program can, if allowed, reconsider the A and M4 chemical compositions making the following changes, which are conservative of the number of electrons deduced from the site occupancy refinement : 1) X atoms of Na in the A site are transformed into $0.579X$ atoms of K with a loss of $0.421X$ positive charges; 2) X atoms of Fe^{2+} and $0.667X$ atoms of Na are introduced into the M4 site at the expense of $1.667X$ atoms of Ca with a loss of $0.667X$ positive charges.

The final CORANF output gives the chemical formula, the comparison between calculated and observed distances, the charge balance between the anionic and cationic portions, and the list of the chemical changes made in order to obtain the best charge balance.

The site population deduced in this way has to be considered, from a general point of view, somewhat arbitrary since it is based upon mean bond distances for pure cations, which can be different in different amphibole series, and upon crystal-chemical assumptions which may need reconsideration in the light of future studies. However, for the amphiboles occurring in the Nybö eclogite pod, both the comparison with the five electron microprobe analyses carried out on the crystals used for the X-ray crystallographic refinement (Table VI), and some correlations between geometric and chemical parameters, suggest that the chemical compositions given in table IV are reasonably reliable.

Further information concerning either the experimental techniques, or those results from the structure refinements or CORANF outputs not tabulated in this paper, may be obtained from the authors.

Sample	Si	Al	Ti	Fe^{3+}	Fe^{2+}	Mg	Ca	Na	K	Name
A4	7.40	1.30	0.03	0.20	0.42	3.82	1.10	1.04	0.07	barroisite
A5	7.40	1.21	0.03	0.22	0.49	3.93	1.01	1.06	0.07	barroisite
B3	7.58	1.05	0.03	0.24	0.36	3.87	1.06	1.03	0.08	winchite
B6	7.64	0.91	0.03	0.26	0.33	3.96	1.05	1.06	0.08	winchite
C1	7.46	1.53	0.02	0.19	0.49	3.44	0.75	1.52	0.05	barroisite
C3	7.55	1.39	0.02	0.11	0.43	3.57	0.82	1.51	0.05	winchite
D6	7.33	1.95	0.02	0.13	0.37	3.20	0.60	1.99	0.03	nyböite
D7	7.48	1.93	0.02	0.04	0.45	3.12	0.45	2.04	0.03	nyböite
D9	7.46	1.82	0.02	0.18	0.31	3.21	0.44	2.13	0.03	nyböite
D18	7.43	1.84	0.02	0.12	0.36	3.23	0.52	2.06	0.05	nyböite
E2	7.24	2.19	0.02	0.23	0.38	2.94	0.33	2.39	0.02	nyböite
E9	7.39	2.08	-	0.13	0.32	3.08	0.39	2.21	0.02	nyböite
E12	7.41	2.10	-	0.14	0.35	3.00	0.24	2.44	0.02	nyböite
E13	7.35	2.13	-	0.17	0.36	2.99	0.34	2.29	0.02	nyböite
E14	7.28	2.16	-	0.17	0.38	3.01	0.47	2.15	0.02	nyböite
E19	7.19	2.21	-	0.12	0.34	3.14	0.45	2.36	0.02	nyböite
E19,1	7.25	2.21	-	0.04	0.40	3.10	0.41	2.40	0.02	nyböite
E19,3	7.22	2.14	-	0.12	0.35	3.17	0.49	2.30	0.02	nyböite
F3	6.24	2.88	0.04	0.50	0.41	2.93	1.06	1.94	-	magnesio-taramite
G2	6.32	2.76	0.04	0.52	0.38	2.98	1.00	2.00	-	magnesio-taramite
H2	6.25	2.80	0.04	0.56	0.49	2.86	1.06	1.94	-	magnesio-taramite

TABLE IV. – *Chemical composition* (from table II) *and names* (see text).

3.3. Electron microprobe analysis

The mean analyses of 5 of the refined amphibole crystals are provided in table V. A Cambridge Microscan V electron microprobe was employed, and for both the wavelength-dispersive-system (WDS) and energy-dispersive-system (EDS) analyses the standards used were : (Co, Zn)F_2 (F), jadeite (Na), periclase (Mg), corundum (Al), wollastonite (Ca, Si), halite (Cl), potassium feldspar (K) and metals (Ti, Cr, Mn, Fe and Ni). Other conditions included a 20 kV accelerating voltage, 30 nA (WDS) and 6 nA (EDS) probe currents, and ZAF correction procedures following Sweatman and Long (1969). A « Kevex series 3000 » Si (Li) detector, « Harwell » pulse-processor, 100 s live-time, and the peak-stripping program of Statham (1976) were used for the EDS analyses.

Sample	A4		C1		D7		E2		F3	
Technique	WDS	EDS	WDS	EDS	WDS	EDS	WDS	EDS	WDS	EDS
Oxide wt. %										
SiO_2	53.26 (.29)	53.04 (.35)	54.17 (.19)	53.55 (.54)	54.51 (.61)	53.79 (.96)	53.84	52.63	43.57 (.40)	43.56 (.16)
Al_2O_3	7.90 (.28)	7.82 (.54)	9.75 (.20)	9.59 (.20)	12.13 (.09)	12.15 (.55)	12.92	13.87	17.66 (.14)	17.94 (.40)
MgO	17.84 (.24)	17.51 (.35)	16.32 (.08)	16.01 (.21)	14.78 (.16)	14.23 (.30)	14.21	13.12	12.65 (.34)	12.79 (.24)
FeO	5.80 (.09)	6.02 (.15)	5.65 (.13)	5.83 (.14)	4.77 (.17)	5.01 (.12)	5.01	5.75	8.27 (.55)	8.13 (.27)
TiO_2	0.24 (.02)	0.24 (.04)	0.21 (.02)	0.14 (.03)	0.17 (.02)	0.15 (.05)	0.16	0.15	0.36 (.06)	0.37 (.08)
Cr_2O_3	0.04 (.02)	n.f.	0.02 (.01)	n.f.	0.02 (.01)	n.f.	n.f.	n.f.	0.00 (.01)	n.f.
MnO	0.03 (.01)	0.10 (.03)	0.03 (.01)	n.f.	0.03 (.02)	n.f.	0.02	0.08	0.13 (.02)	n.f.
NiO	0.11 (.02)	0.13 (.06)	0.11 (.03)	0.11 (.04)	0.13 (.03)	0.18 (.03)	0.11	0.11	0.04 (.03)	n.f.
CaO	7.41 (.05)	7.51 (.12)	5.11 (.07)	5.14 (.09)	3.07 (.03)	3.05 (.04)	2.33	2.75	6.92 (.18)	6.99 (.15)
Na_2O	3.84 (.03)	3.11 (.06)	5.78 (.07)	5.28 (.23)	7.72 (.06)	7.26 (.10)	9.26	8.55	7.07 (.08)	6.65 (.38)
K_2O	0.39 (.01)	0.41 (.08)	0.26 (.01)	0.26 (.07)	0.15 (.03)	0.12 (.07)	0.14	0.11	0.00 (.01)	n.f.
F	0.04 (.01)	n.f.	0.01 (.01)	n.f.	0.02 (.02)	n.f.	n.f.	n.f.	0.01 (.01)	n.f.
Cl	0.03 (.01)	0.02 (.03)	0.02 (.01)	n.f.	0.02 (.01)	n.f.	0.01	0.02	0.01 (.01)	n.f.
- O = F + Cl	0.03	0.00	0.00	0.00	0.01	0.00	0.00	0.00	0.00	0.00
total	96.90	95.91	97.42	95.91	97.51	95.96	98.03	97.14	96.69	96.03

TABLE V. — *Electron microprobe analyses of 5 refined amphiboles;* values are the mean of 3 individual spot analyses with both WDS and EDS except for crystal E2 (1 WDS and 19 EDS analyses), with maximum deviations in parentheses. n.f. = not found.

In general the EDS values give higher Fe and Ca, lower Si, Cr, Mg, Na, Cl, F and total weight %, and similar Al, Ti, Mn, Ni and K to the WDS values. The F and Cl values are somewhat unreliable because of difficulties with the standards. For the trace elements, most of these differences may be attributed to their non-detection by the EDS technique. For the major elements, the differences between mean WDS and EDS analyses are usually less than the differences within the individual WDS or EDS analyses such that these results (*e.g.* Ca) are identical within experimental error. The only significantly large and consistent differences are higher Fe and lower Mg, Na and total. The WDS analyses are usually more precise, as judged by their maximum deviations (Table V), and are presumed to be more accurate, in view of their higher totals, than the EDS analyses. Comparisons are made in section 4 with the analyses by X-ray structure refinement and program CORANF.

An examination of the variation in count rate of Na, K, Ca, Al and Si with continued exposure of these amphiboles to the electron beam has been made in order to evaluate the possibility that alkali loss has affected the analyses (Smith, in prep.). Preliminary results indicate : *a*) significant Na loss, Al and Si gain, but constant K and Ca with time; *b*) in the duration of the actual analyses, maximum expected loss is 0.03 and 0.18 weight % Na_2O by WDS and EDS respectively, and hence is inadequate to explain the much lower Na_2O in the EDS analyses.

4. CRYSTAL CHEMISTRY

4.1. Tetrahedral sites

$\langle T2 - O \rangle$ mean bond lengths for the 21 refined crystal structures (Table III) show very little scatter about their average value (1.630 ± 0.001) in complete agreement with the value obtained for 26 metamorphic blue amphiboles (Ungaretti *et al.*, 1978). The maximum deviation from the average is 0.002 Å which suggests that Al^{IV} is not present in the T2 site of these amphiboles; furthermore this provides an internal criterion for judging the precision of all the other observed mean bond distances.

$\langle T1 - O \rangle$ mean bond lengths range from 1.630 to 1.673 Å indicating significant substitution of Si by Al in the T1 site. The following equation :

$$Al^{IV} \text{ (atoms per f.u.)} = 36.134 \langle T1 - O \rangle - 58.529$$

(Ungaretti, 1980) was used to determine the tetrahedral Al contents, and gave results which are in good agreement with the microprobe analyses (Table VI) and with charge balance requirements of the cationic portion (A + M4 + M1 + M2 + M3) for the crystals belonging to the A, B, C, D and E horizons. However for the F3 magnesio-alumino-taramite (and for the similar amphiboles G2 and H2) the calculated Al^{IV} is significantly higher than that given by the microprobe analysis (1.92 against 1.77 Al^{IV} atoms per f.u.); furthermore assuming 1.92 Al^{IV} atoms, the CORANF computer program failed to give a neutral chemical formula since this needs between 1.80 and 1.70 Al^{IV} atoms. In this regard the equation

$$Al^{IV} = 32.504 \langle T1 - O \rangle - 52.68$$

proposed by Hawthorne and Grundy (1977) gives better results for the taramites suggesting that $\langle T1 - O \rangle$ mean bond lengths can be slightly affected by the chemical composition of the neighbouring sites, mainly by A, M4 and M2.

4.2. A site

Positional disorder of the A site cations has been found in all the amphiboles refined here, as in previous refinements of clinoamphiboles (Papike *et al.*, 1969; Hawthorne and Grundy, 1972, 1973 *a*, *b*, 1978; Hawthorne, 1978 *a*; Robinson *et al.*, 1973). A model involving disorder over the A(2/*m*), A(*m*) and A(2) positions with isotropic temperature factors has been used in all the refinements. The experimental data, characterized by $d(min) = 0.71$ Å, do not allow the obtention of a reliable distribution of the A site cations among the three split positions, since they occur at a distance of 0.5 Å from one another; however the total number of electrons, given by the site occupancy refinement, has proved to be independant from the starting model used and always converged to values which are in very good agreement with WDS microprobe analyses (Table VI) and with

4.3. M4 site

In some of the refined G230*f* amphiboles, the difference Fourier map showed significant residue of electron density in the vicinity of the M4 site, in a position (M4′) characterized by atomic co-ordinates which roughly correspond to those of Fe in cummingtonite (Fisher, 1966) and grunerite (Finger and Zoltai, 1967); this feature has been found in other refined amphiboles (Bocchio *et al.*, 1978) and is very likely due to Fe present in the M4 site which tends to reach a more suitable co-ordination by approaching the oxygens O2, O4, O6 and thus increasing the M4-O5 bond distance. The M4′ site occupancy has been refined by using the Fe scattering factor with the constraint of full occupancy for M4 + M4′. Mg is not considered present in the M4′ position for two main reasons : 1) the available microprobe analyses give in general slightly less Mg and slightly more Fe than that

Sample	Technique	Si	Al	Mg	Fe	Ti	Cr	Mn	Ni	Ca	Na	K	$\Sigma_{cations}$	Σ_{oxide}%	H_2O%
A4	X-ray	7.400	1.300	3.821	0.618	0.026	-	-	-	1.105	1.043	0.068	15.381	97.82	2.18
	WDS	7.398 (0.023)	1.294 (0.049)	3.693 (0.041)	0.674 (0.009)	0.025 (0.002)	0.004 (0.002)	0.004 (0.002)	0.012 (0.002)	1.103 (0.010)	1.034 (0.011)	0.069 (0.002)	15.310	97.18	n.d.
	EDS	7.431 (0.043)	1.292 (0.084)	3.656 (0.070)	0.706 (0.015)	0.025 (0.009)	n.f.	0.012 (0.012)	0.015 (0.015)	1.127 (0.015)	0.845 (0.020)	0.073 (0.012)	15.182	96.23	n.d.
C1	X-ray	7.455	1.535	3.435	0.681	0.024	-	-	-	0.750	1.515	0.046	15.441	97.81	2.19
	WDS	7.439 (0.019)	1.578 (0.033)	3.340 (0.017)	0.648 (0.010)	0.022 (0.002)	0.002 (0.001)	0.003 (0.002)	0.012 (0.003)	0.752 (0.009)	1.534 (0.021)	0.046 (0.006)	15.378	97.70	n.d.
	EDS	7.460 (0.043)	1.575 (0.028)	3.324 (0.053)	0.680 (0.017)	0.015 (0.003)	n.f.	n.f.	0.012 (0.012)	0.767 (0.017)	1.426 (0.058)	0.046 (0.014)	15.304	96.23	n.d.
D7	X-ray	7.484	1.926	3.115	0.487	0.018	-	-	-	0.453	2.037	0.027	15.544	97.80	2.20
	WDS	7.429 (0.039)	1.949 (0.025)	3.002 (0.019)	0.544 (0.023)	0.017 (0.002)	0.002 (0.002)	0.003 (0.002)	0.014 (0.003)	0.448 (0.007)	2.040 (0.028)	0.026 (0.005)	15.475	97.75	n.d.
	EDS	7.440 (0.055)	1.981 (0.102)	2.933 (0.034)	0.582 (0.010)	0.016 (0.005)	n.f.	n.f.	0.020 (0.004)	0.452 (0.010)	1.947 (0.008)	0.021 (0.021)	15.392	96.24	n.d.
E2	X-ray	7.237	2.191	2.944	0.611	0.017	-	-	-	0.326	2.390	0.024	15.740	97.81	2.19
	WDS	7.333	2.075	2.884	0.572	0.016	n.f.	0.002	0.012	0.340	2.445	0.024	15.704	98.30	n.d.
	EDS	7.247 (0.307)	2.252 (0.358)	2.692 (0.200)	0.662 (0.198)	0.016 (0.016)	n.f.	0.009 (0.009)	0.012 (0.012)	0.406 (0.111)	2.283 (0.276)	0.019 (0.019)	15.598	97.44	n.d.
F3	X-ray	6.238	2.882	2.929	0.911	0.040	-	-	-	1.062	1.938	-	15.998	97.89	2.11
	WDS	6.231 (0.031)	2.978 (0.023)	2.696 (0.067)	0.990 (0.070)	0.039 (0.007)	n.f.	0.016 (0.003)	0.005 (0.003)	1.060 (0.030)	1.961 (0.019)	n.f.	15.974	97.13	n.d.
	EDS	6.250 (0.059)	3.035 (0.049)	2.649 (0.053)	0.976 (0.027)	0.040 (0.009)	n.f.	n.f.	n.f.	1.075 (0.016)	1.850 (0.094)	n.f.	15.874	96.48	n.d.

TABLE VI. – *Comparison of the chemical compositions obtained, from the same crystals, by X-ray single-crystal diffractometry and by electron microprobe analysis* per $[O_{22}(OH)_2]$ in all cases; $\Sigma Si + Al + Mg + Fe + Ti - Fe^{2+}_{M4} = 13$ with variable O.S. (oxidation state = $Fe^{3+}/(Fe^{3+} + Fe^{2+})$) by diffraction, and O.S. = 0.5 with variable $\Sigma Si + Al + Mg + Fe + Ti + Cr + Mn +$ Niby microprobe. n.f. = not found; n.d. = not determined; – = assumed absent.

charge balance requirements. Isotropic temperature factors, B, were not constrained and a rather general observed feature was : B(A2*m*) > B(A*m*) > B(A2). The A site occupancy tends to increase through the horizons from A to H in positive relation to the Na content of the co-existing pyroxene (Rossi *et al.*, 1980), reaching full Na occupancy in the F3, G2 and H2 magnesio-alumino-taramites (Table II).

Microprobe analyses of several other amphiboles belonging to eclogite G230 (unpublished data) have shown in general low K contents with a distribution along the A – H horizons of the G230*f* eclogite which changes inversely to that of Na_A (Table II).

obtained by the occupancy refinement of the octahedral sites (Table VI); 2) the M4 and M4′ sites in *C*2/*m* amphiboles have bond distances and co-ordination number which are less unsuitable for Fe^{2+} (and Mn) than for Mg. The Fe^{2+} contents in (M4+M4′) sites have been obtained, only for the 7 crystals with significant M4′ occupancy, by a combination of electron microprobe data, when present, and charge balance considerations; the results range from 0.03 to 0.28 Fe^{2+} atoms per f.u. and occur only in the more calcic amphiboles belonging to the A, B, C and D horizons (Table II). It should be emphasized that the disorder over M4 and M4′

positions can be considered only as an evidence for the presence of Fe^{2+} (or Mn) among the (M4+M4') cations since the M4' site occupancy refinement cannot give reliable Fe^{2+} estimates using 0.71 Å resolution data, with only about 0.6 Å M4 – M4' separation; moreover the possibility that Fe^{2+} is not separated completely from the M4 into the M4' site still remains.

The Na contents in the M4 site, deduced from the occupancy refinement, range from 0.71 to 1.76 atoms per f.u. and increase in a fairly regular way from the A to E horizons, again in positive relation to the Na content of the coexisting pyroxene; in the F, G and H horizons the chemical composition of the M4 site is constant with approximately 1 Na and 1 Ca atoms per f.u. (Table II).

An indirect estimate of the Na present in the M4 site, corroborating very well the results of the occupancy refinement, can be obtained from the *a/c* ratio, which appears to decrease linearly with increasing Na content (Figure 1); the correlation

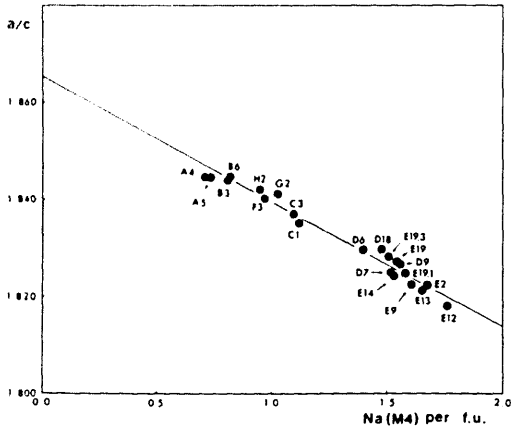

FIG. 1. – *Variation in a/c ratio with the amount of Na at the M4 site;* the equation of the line is: Na(M4) = 72.306 – 38.763 *a/c*, with correlation coefficient $r = 0.994$.

between *a/c* and Na (M4) is rather high for the G230*f* amphiboles since total Fe contents are roughly constant and since the richteritic substitution

$$\square + Ca_2 \rightarrow Na + CaNa,$$

which greatly increases the *a/c* ratio, is not significantly present. Also the sum (*b* + *c*) shows a very high linear correlation with the amount of Na present in the M4 site (Figure 2).

As can be seen from table III, ⟨M4 – O⟩ mean bond distances are not affected by the great changes in the chemical composition of the M4 sites. For the 18 refined amphiboles belonging to the A-E horizons, ⟨M4 – O⟩ has an average value of 2.500 ± 0.002 Å, which significantly differs from that shown by the magnesio-alumino-taramites F, G and H (2.487 ± 0.002 Å). The actual value for the ⟨M4 – O⟩ mean bond distance is greatly affected by the chemical composition of the neighbouring sites; in particular the individual M4 – O5 bond distance shows remarkable

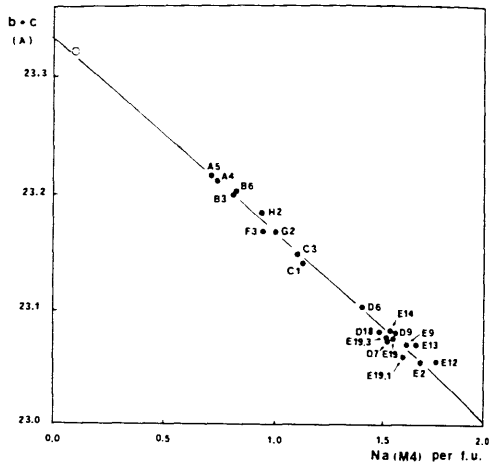

FIG. 2. – *Variation in (b + c) with the amount of Na at the M4 site;* the equation of the line is: Na(M4) = 141.660 – 6.071 (*b* + *c*), with $r = 0.992$. The open circle (not used in calculating the equation) refers to tremolite (Papike *et al.*, 1969).

variations which mainly depend on the amount of Fe present in the octahedral sites (Ungaretti *et al.*, 1978) and on the tetrahedral Al. In figure 3 the variation of the M4 – O5 bond length with ⟨T1 – O⟩ is shown; it is worth noting that the largest difference in M4 – O5 occurs between the amphiboles B6 and F3 which are characterized by a rather similar chemical composition of the M4 site (Table II).

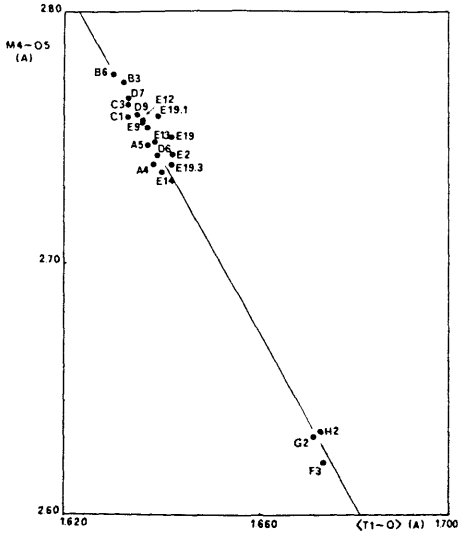

FIG. 3. – *Variation in M4 – O5 bond distance with < T1 – O > mean bond distance;* the equation of the line is: < T1 – O> = 2.431 – 0.289 (M4 – O5), $r = 0.992$.

4.4. Octahedral sites

In all the 21 refined G230 *f* amphiboles the ⟨M2 – O⟩ mean bond length is much shorter than ⟨M1 – O⟩ and ⟨M3 – O⟩ (Table III) indicating a considerable ordering of the trivalent cations at the

M2 site. The ordering is probably incomplete in some crystals, since a small amount of trivalent cations can be attributed, on the basis of the mean bond distances, to the M3 site for the amphiboles belonging to A and B horizons and to M1 for some of the amphiboles belonging to D and E horizons. However trivalent cations have been finally placed only into the M3 site population of some amphiboles; the M1 sites has been considered occupied only by $Mg + Fe^{2+}$ in all the 21 refined amphiboles, both because of total charge balance requirements and because it was observed that when a short $\langle M1 - O\rangle$ mean bond length occurs the corresponding $\langle M3 - O\rangle$ becomes unusually large, irrespective of the Fe content at the M3 site. In the crystal E19, which showed zoning features under the polarizing microscope, this phenomenon was particularly marked, since calculated $\langle M1 - O\rangle$ and $\langle M3 - O\rangle$ mean bond distances for $Mg + Fe^{2+}$ site occupancy were respectively 2.081 and 2.086 Å, against observed values of 2.073 and 2.102 Å. The crystal was broken and two small, apparently homogeneous, fragments (E19,1 and E19,3) were used for new data collection and refinement. The unit cell dimensions (Table I) and the site occupancy refinement (Table II) of the two fragments confirmed the chemical zoning of the original crystal but the same features still affected the $\langle M1 - O\rangle$ and $\langle M3 - O\rangle$ mean bond lengths (Table III).

The unsatisfactory correlation, mainly observed in the amphiboles of the E, F, G and H horizons, between $\langle M1 - O\rangle$ and $\langle M3 - O\rangle$ mean bond lengths and the chemical composition of the M1 and M3 sites (Tables II and III) is not dependent on the chemistry of the O3 site which belongs to both octahedra and which can be occupied by O, F and Cl; in fact no significant F or Cl contents have been detected with the microprobe in the analyzed G230*f* amphiboles ($F + Cl \ll 0.1$ wt. %, table V). Furthermore the difference Fourier map of the 21 refined amphibole structures has shown approximately the same electron density in the expected position for the hydrogen atom and no evidence for significant dehydrogenation was obtained from the inspection of the individual M1 – O3 and M3 – O3 bond lengths, both of which decrease greatly if the substitution of OH^- by O^{2-} occurs at the O3 site (Ungaretti, 1980). It is noteworthy that the average (weighted by their multiplicity) of the observed $\langle M1-O\rangle$ and $\langle M3-O\rangle$ mean bond lengths (2.083 Å) in the crystal E19 is identical to the value calculated assuming that only Mg and Fe^{2+} are present in both sites; this supports the possibility that trivalent cations do not occur in the M1 site such that other structural features, such as cation-cation repulsive interactions and packing constraints (Hawthorne, 1978 *b*), are responsible for the anomalous observed values of $\langle M1-O\rangle$ and $\langle M3-O\rangle$ bond distances. As can be seen from table III all the observed $\langle M1-O\rangle$ mean bond lengths are shorter than the calculated ones for the crystals of the A to E horizons; this may indicate either the presence of small amounts of trivalent cations at the M1 site, as mentioned above, or more likely may indicate that the values for pure Mg and Fe^{2+} cations used for calculating $\langle M1-O\rangle$ and $\langle M3-O\rangle$ mean bond distances and taken from the refinement of the blue amphiboles (Ungaretti *et al.*, 1978) should be slightly adjusted in different amphibole series, since $\langle Mg-O\rangle$ and $\langle Fe^{2+}-O\rangle$ may change if different polyvalent substitutions occur in the neighbouring sites. This latter hypothesis seems to be particularly supported by the F3, G2 and H2 magnesio-alumino-taramites which are characterized by observed octahedral mean bond distances which are all larger than the calculated values.

The result of the influence of the complex pattern of isomorphous substitutions on the size of one octahedral site can be seen in figure 4, where the *b/c* ratio is plotted against the $\langle M2-O\rangle$ mean bond lengths for the 21 refined G230*f* amphiboles; the correlation coefficient is remarkably high ($r = 0.992$) and makes evident the control exerted upon the M2 site by the unit cell dimensions, which themselves certainly reflect the overall chemical composition of the amphibole.

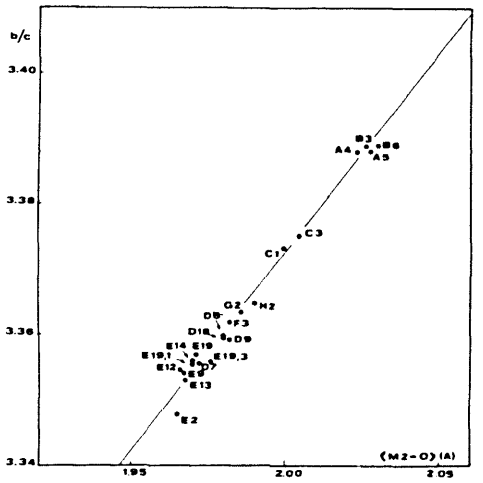

FIG. 4. – *Variation in b/c ration with* $< M2 - O >$ *mean bond distance;* the equation of the line is: $< M2 - O > = 1.629\, b/c - 3.493$, $r = 0.992$.

Finally the $\langle M3-O\rangle$ mean bond distances increase with decreasing $\langle M2-O\rangle$ mean bond lengths (Table III) with a correlation which, even if not particularly high ($r = 0.89$), still suggests that the chemical composition of an octahedral site may not be the main factor in determining its size, since the chemical composition of neighbouring sites can exert a significant influence.

The amount of octahedral iron is rather low and constant (about 0.5 atoms per f.u., table II) in all the amphiboles occurring in the A-E horizons and slightly increases to about 0.9 atoms per f.u. in the F – H magnesio-alumino-taramites. Therefore the main isomorphous substitution occurring in the octahedral sites is $Mg \rightleftharpoons Al^{VI}$. Since the polyvalent substitution $Mg \rightleftharpoons Al^{VI}$ occurs in the M2 site in all the refined amphibole structures, the *b/c* ratio, which is highly correlated with the $\langle M2 - O\rangle$ mean bond distances (Figure 4), can be used to obtain a sufficiently good estimate of Al^{VI}; actually the *b/c* sin β ratio has shown

the highest linear correlation with the Al^{VI} determined by the CORANF computer program following the equation : Al^{VI} (atoms per f.u.) = 76.459 − 14.488 (b/c sin β), with a correlation coefficient r = 0.991.

Many other linear correlations between geometric parameters and chemical compositions have been found for the G230*f* amphiboles; one of these is shown in figure 5 and relates the T1 − O5 − T2 angle to the total $Al^{IV} + Al^{VI}$ contents; with the Al^{VI} estimate confirmed by the b/c sin β ratio, the linear relationship of figure 5 represents a good test for the

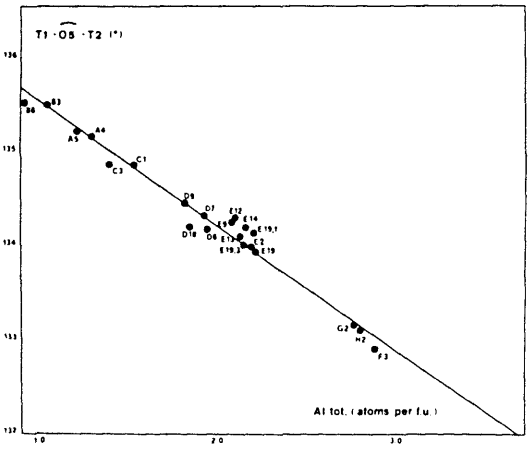

FIG. 5. – *Variation in T1 − O5 − T2 angle with the total aluminum contents;* the equation of the line is : $(Al^{VI} + Al^{VI}) = 102.988 - 0.752$ (T1 − O5 − T2), $r = 0.985$.

reliability of the Al^{IV} estimate based upon the ⟨T1−O⟩ mean bond distances. The T1 − O5 − T2 angle is also correlated with the unit cell dimensions, particularly with the $(a+b)/c$ ratio with a correlation coefficient r = 0.97. Therefore a rough estimate of the chemical composition of the G230*f* amphiboles, characterized by rather constant iron contents, can be obtained by appropriate combinations of the unit cell dimensions alone.

4.5. Nomenclature

In table IV the chemical compositions of the refined G230*f* amphiboles per $[O_{22}(OH)_2]$ and

$$\Sigma Si + Al + Mg + Fe + Ti - Me^{2+}_{M4} = 13,$$

derived from program CORANF, are reported together with their names given according to the system « Nomenclature of Amphiboles » by the I.M.A. Subcommittee on Amphiboles (Leake *et al.*, 1978).

All the crystals from the D and E horizons are alkali amphiboles on the basis of $Na_{(M4)} > 1.34$; within the alkali amphibole group they are closest in composition to the only remaining un-named end-member of the 13 possible in the system :

$$Na_{0-1}(Ca, Na)_2Mg_{3-5}Al_{0-2}Si_{6-8}Al_{0-2}O_{22}(OH)_2.$$

Recognition of the name « nyböite » for the amphibole with the ideal chemical formula

$$NaNa_2Mg_3Al_2Si_7AlO_{22}(OH)_2$$

is under consideration by the I.M.A. Commission on New Minerals and Mineral Names.

The crystals from the F, G and H horizons are clearly closest in composition to the magnesio-alumino-taramite end-member

$$NaCaNaMg_3Al_2Si_6Al_2O_{22}(OH)_2.$$

These are the first recorded compositions closest to this end-member, since the only taramites previously known have $Fe^{2+} > Mg$ and $Fe^{3+} > Al^{VI}$, such that the Nybö eclogite pod provides a second new amphibole.

In fact, in several cases the names which we are obliged to give are not those of the closest end-member in 4-dimensional amphibole compositional space (*e.g.* $(K + Na)_A$, Na_{M4}, $(Al^{VI} + Fe^{3+})_{oct.}$ and Al^{IV}_T, Smith and Ungaretti, in prep.). In particular none of the amphiboles are closest to barroisite; for example crystal A4 is actually closest to winchite as is suggested by the projection of the M4 and octahedral site variables in figure 8 but is obscured in the projection of the A and T site variables in figure 7. Similarly crystals D6 and D18 with $1.34 < Na_{M4} < 1.50$ are actually closest to magnesio-alumino-katophorite rather than nyboïte (Figures 6 and 8). These anomalies coullbe resolved : (I) by the *simultaneous* consideration of all the four principal substitutions in 4-dimensional amphibole compositional space, instead of the *consecutive* consideration of the M4, A and T site variables with disregard of the equally important octahedral site variable; and (II) by consistently using 0.5 and 1.5 atomic units for all four variables for the basic name boundaries, instead of 0.5 and 1.5 for the A and T variables but 0.67 and 1.34 for the M4 variable, and unspecified atomic units for the octahedral site variable.

5. THE AMPHIBOLE COMPOSITION RANGE AND ITS RELATIONSHIP TO THE LOCAL BULK-ROCK CHEMICAL COMPOSITION

In the plot of the sum of the high charge cations in the octahedral sites against Al^{IV}, provided in figure 6, using the individual site populations by structure refinement given in table II, the data points tend to cluster into three groups : A + B + C (« barroisites » and winchites), D + E (nyböites) and F + G + H (magnesio-alumino-taramites). The distribution partly reflects a sampling bias in searching for more nyböites and we doubt that the apparent small gap between the groups A + B + C and D + E is real since there is a continuity in the variation of the unit cell dimensions from horizon A to E (Table VII), in petrography (*e.g.* all are garnet-bearing) and in the isomorphous substitution

$$\square + Si_{T1} \rightarrow (Na, K)_A + Al^{IV}_{T1} \text{ (Figure 7).}$$

Horizon	crystals measured	a (Å)	b (Å)	c (Å)	β (°)	V (Å^3)
A	4	9.760 (3)	17.927 (7)	5.289 (1)	104.45 (4)	896.1
B	5	9.747 (6)	17.913 (2)	5.289 (1)	104.30 (3)	894.8
C	3	9.719 (8)	17.857 (5)	5.292 (2)	104.21 (2)	890.3
D	7	9.671 (14)	17.780 (16)	5.297 (3)	104.11 (6)	883.3
E	23	9.667 (22)	17.775 (12)	5.299 (4)	104.15 (8)	882.9
F	2	9.766 (9)	17.835 (25)	5.312 (8)	104.82 (1)	894.5
G	2	9.773 (7)	17.859 (3)	5.312 (4)	104.79 (4)	896.4
H	2	9.787 (1)	17.869 (8)	5.313 (8)	104.88 (5)	897.9

TABLE VII. – *Unit cell dimensions obtained by averaging the values measured upon crystals belonging to the same horizon;* parenthesized figures represent the estimated standard deviations in terms of least units cited for the value to their immediate left.

The composition gap between the magnesio-taramites and the other groups is more distinct (see figures 6, 7 and 8), and is wider, and is accompanied by petrographic changes (symplectitic instead of early amphiboles, garnet absent, and higher amphibole mode 0.2-2 %), such that the gap is considered real. This gap may thus be attributed to the different P – T – time conditions of formation of the early and symplectitic amphiboles, but there could also be an immiscibility region here.

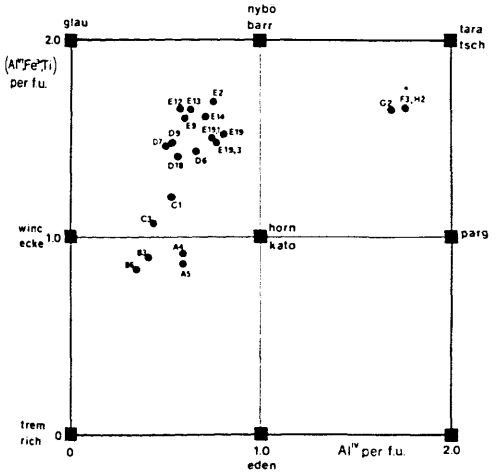

FIG. 6. – *Plot of high charge octahedral cations vs. tetrahedral aluminum.*

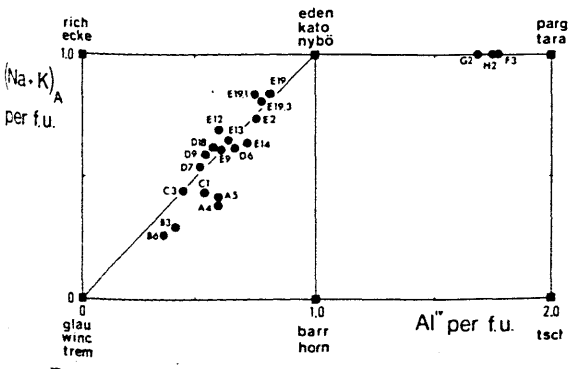

FIG. 7. – *Plot of the tetrahedral aluminum vs. the sum of the cations at the A site.*

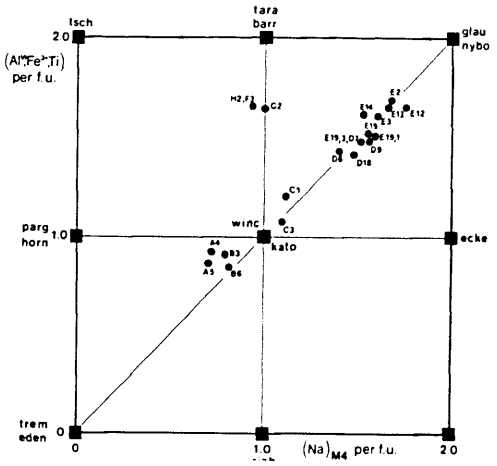

FIG. 8. – *Plot of the high charge octahedral cations vs. the amount of Na at the M4 site.*

The bulk chemistry is dominated by clinopyroxene since it comprises > 99.9 % of the volume of non-amphibolitised parts of horizons F, G and H, and it comprises about 50 % of the volume of the garnet-bearing horizons A – E.

Over 200 electron microprobe analyses of the clinopyroxenes (Carpenter and Smith, 1981; Rossi *et al.*, in prep.) show that they all plot close to a straight line in multi-dimensional pyroxene compositional space, since they reflect a near-perfect substitution between jadeite and diopside with low and almost constant total Fe. Hence any chemical parameter will reflect the clinopyroxene compositional variation, but X_{Na} seems particularly appropriate. Several choices are available for representing the amphibole compositional variation; figure 9 plots X_{Na} in amphiboles against X_{Na} in clinopyroxenes (Na for amphiboles includes both the A and M4 sites; the mean X_{Na} values of each horizon are plotted); the figure clearly shows an excellent trend in horizons A – E which is compatible with the formation of early amphiboles essentially by the hydration of primary pyroxene (Smith, 1971, 1976; Lappin and Smith, 1978). Thus we may deduce that the amphibole compositional range between « barroisite », winchite and nyböite is directly a function of the local bulk chemical environment at constant, or almost constant, P – T conditions. More specifically the isomorphous substitution

$$Ca_{M4} + Mg_{M2} \rightarrow Na_{M4} + Al_{M2},$$

which also characterizes the amphiboles belonging to the A – E horizons (Figure 8) is identical to the substitution from diopside to jadeite. Thus the trend in horizons A – E of figure 9 shows a near-perfect linear relationship between parent (pyroxene) and daughter (amphibole). Replotting figure 9 with only Na_{M4} in X_{Na} in amphibole yields a similarly-good near-parallel trend.

Figure 9 suggests a significant difference in the control of the amphibole composition from E to F, G and H, and also that the linear trend from A to E is not just a function of Na in clinopyroxene, since Na

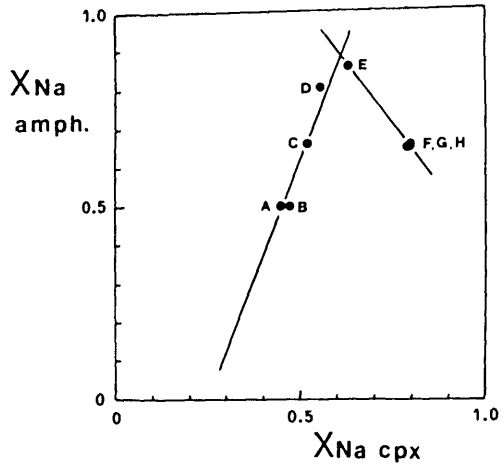

FIG. 9. — *Plot of $X_{Na} = Na/(Ca + Na)$ in the amphiboles vs. the corresponding value in the coexisting pyroxenes;* the points represent the mean value of X_{Na} obtained from crystals belonging to the same horizon.

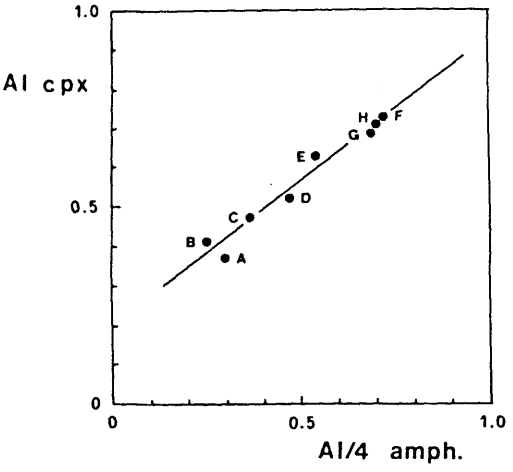

FIG. 10. — *Plot of the total amount of Al (referred to 6 oxygen atoms) in the amphiboles vs. the corresponding value in the coexisting pyroxenes;* the points represent the mean value of Al(tot) obtained from crystals belonging to the same horizon.

becomes enriched in the amphiboles from A to E and abruptly becomes relatively depleted from E to F, G and H. Figure 10, which plots total Al (pyroxene) versus total Al (amphibole), reveals that Al is the controlling factor, since the linear trend from A to E continues linearly to F, G and H.

The slight differences in composition between crystals A4 and A5 and the major trend in horizons B – E (Figures 6-10) may be attributed to incipient amphibolitisation having caused minor chemical adjustment from the original composition of « early » amphiboles A4 and A5 towards compositions typical of « symplectitic » amphiboles (section 2), in particular higher Al^{IV} (Figures 6 and 7), as is observed in several other eclogites (Lappin and Smith, 1978 and in prep.). This is supported by the lower Na_{M4} in A4 and A5 and the fact that the direction of the principal compositional substitution from horizons B and C

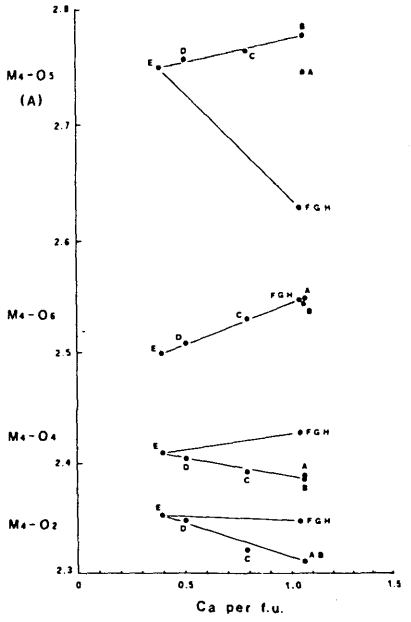

FIG. 11. — *Variation in the individual M4 – O bond distances with the chemical composition of the M4 site.* Each point represents the mean value of the M4 – O bond distances obtained from crystals belonging to the same horizon.

to A ($Na_{M4} + Si_{T1} \rightarrow Ca_{M4} + Al^{IV}_{T1}$) is identical to that from the « early » amphiboles in horizon E to the « symplectitic » amphiboles in horizons F, G and H (Figures 6, 7 and 8). Furthermore in terms of certain bond distances, crystals A4 and A5 suggest some affinity with the truly symplectitic amphiboles in horizons F, G and H (*e.g.* M4 – O5, figure 11).

We may therefore explain the data as follows. From A to E, Al enters the octahedral M2 site and charge balance is compensated by Na entering the M4 site, in an analogous fashion to the polyvalent isomorphous substitution $Ca + Mg \rightarrow Na + Al^{VI}$ shown by the parent pyroxenes (Lappin and Smith, 1978; Carpenter and Smith, 1981; Rossi *et al.*, in prep.). Since in pyroxenes all the compositions between diopside and jadeite can be stable at high P and medium T (Smith *et al.*, 1980), given appropriate bulk chemical compositions, whilst only jadeite-poor pyroxenes can be stable at low P and medium T, we thus deduce that the whole range of amphibole compositions from A to E can be stable at high P, whilst only the nyböite-poor amphiboles can be stable at low P.

It is relevant to note here that a broadly similar range of winchite to « barroisite » amphibole compositions is achieved by high pressure metamorphism ($\geqslant$ 15 kbar) in the Sesia-Lanzo Zone (Domeneghetti *et al.*, in prep.) and that this range is again dependent upon the local bulk chemical composition at probably constant P – T conditions. Thus there is evidence for the pressure conditions required to stabilize winchite to « barroisite » compositions in the Sesia-Lanzo amphiboles formed by increasing pressure, and in the Nybö amphiboles most probably formed by decreasing pressure (15-28 kbar approached from 30-40 kbar estimated for several eclogite pods including that at Nybö; Lappin and Smith, 1978 and in prep.). This further supports

the metamorphic similarity of the high-pressure event in these particular units within the Alpine and Caledonian orogenic belts deduced by analogies in other mineral groups (*e.g.* Na + Al clinopyroxenes, phengites, and F + Al sphenes: Smith, 1980 *a*, *c*). The principal difference between these geological units is the higher T of the Nybö eclogite (700-850 °C) which allowed the formation of nyböite ($0.5 < Al^{IV} < 1.0$) and prevented the formation of glaucophane ($Al^{IV} \approx 0.0$), whilst the lower T of the Sesia-Lanzo eclogites (≈ 550 °C) allowed the formation of glaucophane.

As the end-member composition nyböite

$$NaNa_2Mg_3Al_2Si_7AlO_{22}(OH)_2$$

is approached, the M2 site becomes highly enriched in Al and the repulsive interactions responsible for the anomalous small $\langle M1-O\rangle$ and large $\langle M3-O\rangle$ mean bond distances may prevent filling of the M2 site by the relatively small Al^{VI} cation. Likewise the

$$Ca_{M4} + Mg_{M2} \rightarrow Na_{M4} + Al^{VI}_{M2}$$

exchange (Figure 8) is arrested because the M4 site is nearly full of Na, and Na cannot go into the A site since that is also nearly full because of the substitution

$$\square + Si_{T1} \rightarrow Na_A + Al^{IV}_{T1},$$

which simultaneously increases from the A to E horizons (Figure 7). Above horizon E, further Al, as provided by the parent pyroxene, can only go into the T1 site but cannot be accompanied by additional Na in the A site for the reason mentioned above. Of necessity Na must leave the M4 site according to the exchange

$$Na_{M4} + Si_{T1} \rightarrow Ca_{M4} + Al^{IV}_{T1},$$

which takes the composition directly towards magnesio-alumino-taramite

$$NaCaNaMg_3Al_2Si_6Al_2O_{22}(OH)_2,$$

hence the abrupt change of slope in figure 9 but continuous slope in figure 10.

The large jump between amphibole compositions in horizons E and F, G and H (Figures 6, 7 and 8) can be explained as the result of a wide miscibility gap necessitated by local charge balance and bond distance requirements. Thus additional entry of Al into the T1 site requires a different pattern of local charge balance, implying a complete re-arrangement of the individual bond distances; an example of this is shown in figure 11, where the mean values of the individual M4 – O bond distances are plotted against Ca (M4). It is quite clear that M4 – O bond distances change almost linearly going from the A to the E horizon and that they greatly deviate, especially M4 – O5, from the previous trend as soon as the chemical composition of the M4 site comes back towards sodic-calcic amphiboles. The same situation also occurs in the M1 and M2 sites, whose individual M – O bond distances show a large re-arrangement going from the E to the F, G and H horizons. The latter structural arrangement is probably prevented by very high pressure conditions and by the conflicting chemical control (increasing Al *and* increasing Na) exerted by the parent pyroxenes, in such a way that no amphiboles can form in the F, G and H horizons if the P – T conditions remain the same as those prevailing during the crystallization of nyböite. This explains why we have not found any early amphiboles in the F, G and H horizons.

We hypothesise that a moderate release of pressure in the presence of a sufficiently high temperature (P = 9-13 kbar and T = 650-720 °C estimated by Lappin and Smith, 1978) might allow the required structural arrangements and the formation of magnesio-alumino-taramite.

High Fe in the M2 site very likely assists the stabilization of the taramite structure, which is in fact characterized by a slightly expanded octahedral strip, as can be deduced by the comparison between observed and calculated mean bond distances given in table III. This may explain why the Nybö taramites belonging to the horizons F, G and H have higher Fe than the other amphiboles (Table IV) and than the parent pyroxenes, *i.e.* they have effectively drawn in Fe from the environment. The same consideration suggests that pure magnesio-alumino-taramite may not be stable in nature and explains why the ferro-ferri-end-member is the only taramite normally found as this would be more stable.

In fact the only ferro-ferri-taramites known, previously named as « mboziite » or « sundiusite » or other, less appropriate, names, all occur in subsilicic K-, Na- and Al-rich igneous rocks, apart from one significant exception : an Mg- and Al-rich « mboziite » (Linthout and Kieft, 1970) which nevertheless still lies in the ferro-ferri-taramite field since $Mg < Fe^{2+}$ and $Al^{VI} < Fe^{3+}$. The important correlation between the regional metamorphic origin of this relatively Mg- and Al-rich taramite in contrast to the igneous origin of the Fe^{2+}- and Fe^{3+}-rich taramites (cf the relation between glaucophanes and riebeckites) was noted by Linthout and Kieft (1970). Thus one may expect Mg- and Al-richer taramites in relatively high P/low T metamorphic rocks.

This leads us to further conclude that magnesio-alumino-taramites require exceptional chemical conditions (extremely-high Al, high Na and low Fe) as well as moderately high pressure, such as provided by the Nybö eclogite pod. This accounts for the examples, so far unique, of both magnesio-alumino-taramite and nyböite at Nybö, since both require essentially the same chemical conditions, but nyböite also requires yet higher pressures (*e.g.* Smith, 1980 *a*, *b*) than the amphibolite-facies symplectitic magnesio-alumino-taramites and the co-facial enveloping gneisses.

ACKNOWLEDGEMENTS

D.C.S. acknowledges the Natural Environment Research Council and the University of Edinburgh, U.K., for provision of the electron microprobe facilities. We are grateful to Professor J. Fabriès for a critical reading of the manuscript.

Reçu le 5 juillet 1980
Accepté le 11 décembre 1980

REFERENCES

BOCCHIO, R., UNGARETTI, L. and ROSSI, G. (1978). – Crystal-chemical study of eclogitic amphiboles from Alpe Arami, Lepontine Alps, Southern Switzerland. *Rendiconti Soc. Ital. Mineral. Petrol., 34,* 453-470.

CARPENTER, M. A. and SMITH, D. C. (1981). – Solid solution and cation ordering limits in high temperature sodic pyroxenes from the Nybö eclogite pod, Norway. *Mineral. Mag., 44,* 37-44.

FINGER, L. W. and ZOLTAI, T. (1967). – Cation distribution in grunerite. *Trans. Amer Geophys. Union, 48,* 233-234.

FISCHER, K. F. (1966). – A further refinement of the crystal structure of cummingtonite. *Amer. Mineral., 51,* 814-818.

HAWTHORNE, F. C. (1978 *a*). – The crystal chemistry of the amphiboles. VIII. The crystal structure and site chemistry of fluor-riebeckite. *Can. Mineral., 16,* 187-194.

HAWTHORNE, F. C. (1978 *b*). – The crystal chemistry of the amphiboles. VI. The stereochemistry of the octahedral strip. *Can. Mineral., 16,* 37-52.

HAWTHORNE, F. C. and GRUNDY, H. D. (1972). – Positional disorder in the A-site of clinoamphiboles. *Nature, 235,* 72-73.

HAWTHORNE, F. C. and GRUNDY, H. D. (1973 *a*). – The crystal chemistry of the amphiboles. I. Refinement of the crystal structure of ferro-tschermakite. *Mineral. Mag., 39,* 36-48.

HAWTHORNE, F. C. and GRUNDY, H. D. (1973 *b*). – The crystal chemistry of the amphiboles. II. Refinement of the crystal structure of oxy-kaersutite. *Mineral. Mag., 39,* 390-400.

HAWTHORNE, F. C. and GRUNDY, H. D. (1977). The crystal chemistry of the amphiboles. III. Refinement of the crystal structure of a sub-silicic hastingsite. *Mineral. Mag., 41,* 43-50.

HAWTHORNE, F. C. and GRUNDY, H. D. (1978). – The crystal chemistry of the amphiboles. VII. The crystal structure and site chemistry of potassian ferri-taramite. *Can. Mineral., 16,* 53-62.

International Tables for X-Ray Crystallography (1974), The Kynoch Press, Birmingham, 99-102.

LAPPIN, M. A. and SMITH, D. C. (1978). – Mantle-equilibrated orthopyroxene eclogite pods from the basal gneisses in the Selje District, Western Norway. *J. Petrol., 19,* 530-584.

LAPPIN, M. A. and SMITH, D. C. (1981). – Carbonate-silicate relationships in some eclogites from Sunnmore and Nordfjord, Norway. *Trans. R. Soc. Edinburgh, Earth Sciences,* (in press).

LEAKE, B. E. *et al.* (1978). – Nomenclature of Amphiboles. *Bull. Minéral., 101,* 453-467.

LINTHOUT, K. and KIEFT, C. (1970). – Preliminary note on a mboziite of metamorphic origin. *Mineral. Mag. 37,* 629-631.

NORTH, A. C. T., PHILLIPS, D. C. and MATHEWS, F. S. (1968). – A semi-empirical method of absorption correction. *Acta Cryst., A24,* 351-359.

PAPIKE, J. J., ROSS, M. and CLARK, J. R. (1969). – Crystal-chemical characterization of clinoamphiboles based on five new structure refinements. *Mineral. Soc. Amer. Spec. Paper 2,* 117-136.

ROBINSON, K., GIBBS, G. V., RIBBE, P. H. and HALL, M. R. (1973). – Cation distribution in three hornblendes. *Amer. J. Sci., 273A,* 522-535.

ROSSI, G., UNGARETTI, L., MOTTANA A., SMITH, D. C. and DOMENEGHETTI, C. (1980). – Chemical variation and cation ordering in Na-rich to Na-poor clinopyroxenes from the Nybö eclogite pod, Nordfjord, Norway : investigation by structure refinement and electron microprobe analysis. *Abstracts, 12th I.M.A. General Meeting, Orléans,* 187.

SMITH, D. C. (1971). – A tourmaline-bearing eclogite from Sunnmöre, Norway. *Norsk. Geol. Tidsskr., 51,* 141-147.

SMITH, D. C. (1976). – The geology of the Vartdal area, Sunnmöre, Norway, and the petrochemistry of the Sunnmöre eclogite suite. Unpublished Ph. D. Thesis, University of Aberdeen.

SMITH, D. C. (1978). – The eclogite/amphibolite transition in the Caledonide Orogen in West Norway and East Greenland. *Abstracts, I.G.C.P. Caledonide Conference,* University of Dublin, 54.

SMITH, D. C. (1980 *a*). – Exceptional mineral compositions in very high pressure hydrous-eclogite-facies paragenes-es in the Precambrian suite of eclogite lenses in the Selje and Vartdalsfjorden Districts of the Basal Gneiss Region, S. W. Norway. *Abstracts, 26th International Geological Congress, Paris, section 01.3.3,* 92.

SMITH, D. C. (1980 *b*). – A tectonic melange of foreign eclogites and ultramafites at Lien, and elsewhere, in the Basal Gneiss Region, West Norway. *Nature, 287,* 366-368.

SMITH, D. C. (1980 *c*). – Highly aluminous sphene (titanite) in natural high pressure hydrous-eclogite-facies rocks from Norway and Italy, and in experimental runs at high pressure. *Abstracts, 26th International Geological Congress, Paris, section 02.3.1.* 145.

SMITH, D. C., MOTTANA, A. and ROSSI, G. (1980). – Crystal-chemistry of a unique jadeite-rich acmite-poor omphacite from the Nybö eclogite pod, Sörpollen, Nordfjord, Norway. *Lithos, 13,* 227-236.

STATHAM, P. J. (1976). A comparative study of techniques for the quantitative analysis of the X-ray spectra obtained with Si(Li) detector. *X-Ray Spectrom., 5,* 16.

SWEATMAN, P. J. and LONG, J. V. P. (1969). – Quantitative electron-probe microanalysis of rock-forming minerals. *J. Petrol., 10,* 332-379.

UNGARETTI, L. (1980). – Recent developments in X-ray single crystal diffractometry applied to the crystal-chemical study of amphiboles. *Proceedings of the 15th Conference of the Yugoslav Centre of Crystallography. Bor,* in press.

UNGARETTI, L., MAZZI, F., ROSSI, G. and DAL NEGRO, A. (1978). – Crystal-chemical characterization of blue amphiboles. *Proceedings of the 11th I.M.A. General Meeting, Novosibirsk,* in press.

Erratum : M3 – O calc for sample E 12 in table III should read 2.083 instead of 2.087.

Addenda en date du 6 mai 1981 : This new mineral and its name nyboïte have been approved by the Commission on New Minerals and Minerals Names of the I.M.A. (September 1980).